Relating volcano morphometry to the developmental progression of Hawaiian shield volcanoes through slope and hypsometric analyses of SRTM data

Jacob E. Bleacher[1,2] and Ronald Greeley[1]

Received 24 July 2006; revised 24 April 2008; accepted 6 May 2008; published 19 September 2008.

[1] We calculated average and median slope values and produced hypsometric curves for the subaerial Hawaiian shield volcanoes using Shuttle Radar Topography Mission (SRTM) digital elevation models. The SRTM-derived average and median slope values display similar trends to published results based on other topographic data products, showing an increase in slope relative to volcano age. Shadows in the radar data over high relief regions reduce the slope values calculated for older volcanoes that have undergone significant erosion as compared to nonradar topographic data, suggesting that SRTM data are less sensitive to studies of erosion. Both the 1 and 3 arc sec SRTM data provide comparable results showing that the nearly global 3 arc sec data can be used to conduct the same studies for other volcanoes. Hypsometric analyses show that the Hawaiian shields maintain consistent upward and lateral growth until alkalic capping and subsidence alter the relief-surface area ratio. Changes in the morphology of the Hawaiian volcanoes are in part related to decreased magma production rates at older shields. The internal dynamics act to decrease the steadiness and duration of magma delivery to the surface causing a decrease in buffered eruptions and lava tube formation, all of which contribute to an increase in slope and relief-surface area ratios. Terrain analyses combined with mapping can provide insight into the development of remote volcanoes or volcanoes on other planets for which remotely sensed data exist but less is known about their internal and eruptive history.

Citation: Bleacher, J. E., and R. Greeley (2008), Relating volcano morphometry to the developmental progression of Hawaiian shield volcanoes through slope and hypsometric analyses of SRTM data, *J. Geophys. Res.*, *113*, B09208, doi:10.1029/2006JB004661.

1. Introduction

[2] The Hawaiian shield volcanoes are among the best studied volcanoes on Earth [*Tilling and Dvorak*, 1993]. A generalized developmental sequence for these shield volcanoes includes: (1) an initial alkalic stage, (2) a tholeiitic shield building stage, (3) an alkalic capping stage, and (4) an erosion stage [*Clague and Dalrymple*, 1987; *Peterson and Moore*, 1987]. The subaerial parts of the shield volcanoes Kilauea, Mauna Loa, Hualalai, Mauna Kea, and Kohala (in order of increasing age, shown in Figure 1) represent stages two through four. Because of their age progressive nature (increasing in age and developmental stage to the northwest) they provide insight into how shield volcanoes might evolve through their constructive and erosive history. One of the primary goals of studying these volcanoes is to link subsurface magmatic and tectonic processes to the surface processes and resultant morphologies in order to gain insight into the dynamics of basaltic shield-style volcanism [*Tilling and Dvorak*, 1993]. This is required not only to understand the Hawaiian system but also to serve as a framework for interpreting other basaltic systems for which fewer data are available.

[3] The quantitative representation of surface topography, known as morphometry, is an integral component in the exploration of the Earth and other planets [*Pike*, 2000]. Terrain analysis includes a variety of techniques to quantify the processes that build and modify landscapes [*Wilson and Gallant*, 2000; *Pike*, 2000]. Traditionally, terrain analyses have been used to classify the interaction between tectonic construction and erosive destruction of a landscape [*Wilson and Gallant*, 2000]. However, the surface form of the Hawaiian shields results mostly from volcanic construction and erosive destruction and therefore can provide clues about its volcanic evolution [*Mark and Moore*, 1987; *Moore and Mark*, 1992; *Rowland and Garbeil*, 2000]. The complete coverage of Hawaii by the Shuttle Radar Topography Mission (SRTM) [*Rodriguez et al.*, 2005; *Farr et al.*, 2007] provides an opportunity to compare these data with past studies and to assess new terrain analysis techniques.

[4] *Mark and Moore* [1987], *Moore and Mark* [1992], and *Rowland and Garbeil* [2000] illustrated the validity of conducting average slope-elevation studies for the Hawaiian

[1]School of Earth and Space Exploration, Arizona State University, Tempe, Arizona, USA.
[2]Planetary and Geodynamics Laboratory, NASA Goddard Space Flight Center, Greenbelt, Maryland, USA.

Copyright 2008 by the American Geophysical Union.
0148-0227/08/2006JB004661$09.00

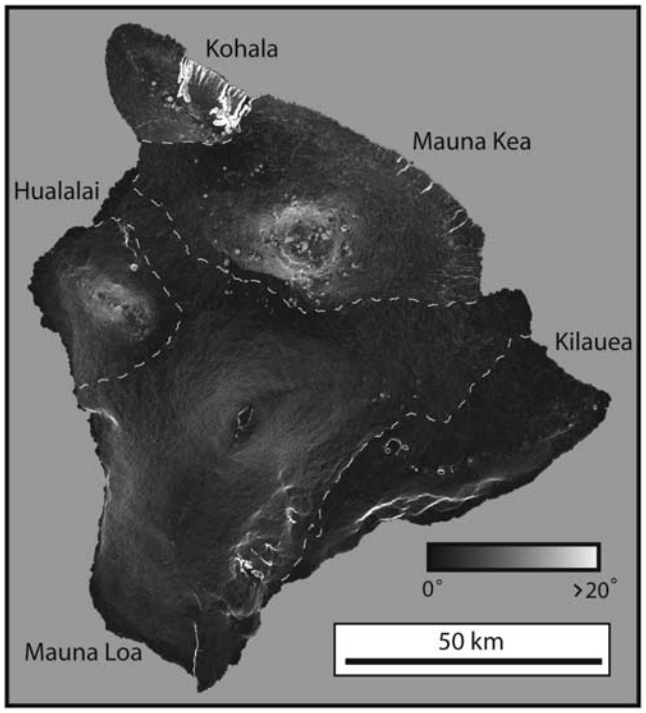

Figure 1. Slope data for the five shield volcanoes of Hawaii. Volcano boundaries are indicated by dashed white lines and are based on the mapped volcano boundaries of *Wolfe and Morris* [1996].

shields based on digital elevation models (DEM). Additionally, *Rowland and Garbeil* [2000] stated that as new digital topographic data are collected, the use for quantitative studies of volcanoes will increase and evolve. The objective of our study was to assess the usefulness of the SRTM data products by comparing the trend in average and median slope values among the Hawaiian volcanoes with the results of *Moore and Mark* [1992] and to apply an additional terrain analysis technique, hypsometry, to contribute insight into the development of shield volcanoes. Both techniques provide a quantitative assessment of the slope of each volcano, enabling morphometric comparisons between shields at different stages of development. Futhermore, we show that the SRTM data, which are available for the Hawaiian shields at both 1 and 3 arc sec (~30 and 90 m per pixel, respectively), enables an assessment of the scale dependency of our results. We conclude this paper by correlating our results with other trends related to the development of the Hawaiian shields so that similar studies conducted for other shields can be used to provide insight into their evolution.

2. Background

2.1. Previous Work

[5] *Mark and Moore* [1987] showed that slope analysis can be related to the constructive and destructive history of volcanic terrains. Their approach was to plot average slope against 100 m elevation bands for the subaerial and submarine flank of the Hawaiian Ridge derived from topographic and bathymetric data. They determined that at the scale of 750 m/pixel, subaerial slopes are typically 3° to 6° with slopes increasing at higher elevations to 9° to 13° for older shields.

[6] *Moore and Mark* [1992] and *Rowland and Garbeil* [2000] used DEMs derived from orthophoto quads, stereo photographs, and topographic maps to conduct the same approach, but at a resolution of 30 m/pixel. By plotting slope against elevation they were able to identify areas on each volcano that showed the effects of nonvolcanic processes. For example, both Kohala and Kilauea display higher than average slopes in their lower elevation ranges due to fluvial erosion and mass movements. By removing these data, *Rowland and Garbeil* [2000] showed that each shield (except for Kilauea where slopes show little change with elevation) displays a consistent, low slope at its lower elevation distal margins, and increasing slopes at higher elevations. The older shield volcanoes show a larger slope increase at high elevation. *Moore and Mark* [1992] also presented average slope values of each volcano to show that older volcanoes display higher slopes.

[7] Results led both groups to conclude that the increase in slope is related to eruption conditions, including the transition from eruption of fluid tholeiitic lavas from the summit or along rift zones during the shield building stage (Kilauea and Mauna Loa), to eruption of volatile-rich alkalic lavas from many individual source vents located around the summit during the capping stage (Hualalai and Mauna Kea). The highest slopes were determined to be related to erosion. These morphometric studies established a basis for continued application of previously tested techniques to assess the usefulness of new data.

2.2. Shuttle Radar Topography Mission

[8] The SRTM was a collaboration between the National Aeronautics and Space Administration and the National Geospatial-Intelligence Agency. During February 2000 space shuttle *Endeavor* collected fixed baseline, dual frequency (C-band and X-band) interferometric radar data with nearly global coverage (http://www2.jpl.nasa.gov/srtm/). The C-band data were processed at the Jet Propulsion Laboratory to produce a digital topographic grid between 60°N and 56°S at a 3 arc sec spatial resolution (~90 m/pixel) and a 1 arc sec grid (~30 m/pixel) for the United States [*Rabus et al.*, 2003; *Rodriguez et al.*, 2005; *Farr et al.*, 2007]. The resulting SRTM-derived DEM provides orthometric elevation in meters within the WGS84 reference system with respect to the EGM96 geoid (http://www2.jpl.nasa.gov/srtm/).

[9] In a report on the overall accuracy of the data, *Rodriguez et al.* [2005, 2006] state that the horizontal and vertical accuracies meet and exceed the mission requirements of 20 m (circular error at 90% confidence) and 16 m (linear vertical error at 90% confidence) for the global data, with results for North America yielding mean vertical errors of -0.8 ± 8.3 m (±8.5 m at 90% confidence). *Carabajal and Harding* [2005] performed an error assessment based on comparison with the Geoscience Laser Altimeter System (GLAS) on board the Ice, Cloud, and Land Elevation Satellite (ICESat) and determined that SRTM error is, in part, dependent on the degree of local relief and vegetation ranging from -0.60 ± 3.46 m (low relief, low vegetation) to -5.61 ± 15.68 m (high relief, high vegetation). *Falorni et al.* [2005] and *Guth* [2006] determined that radar speckle

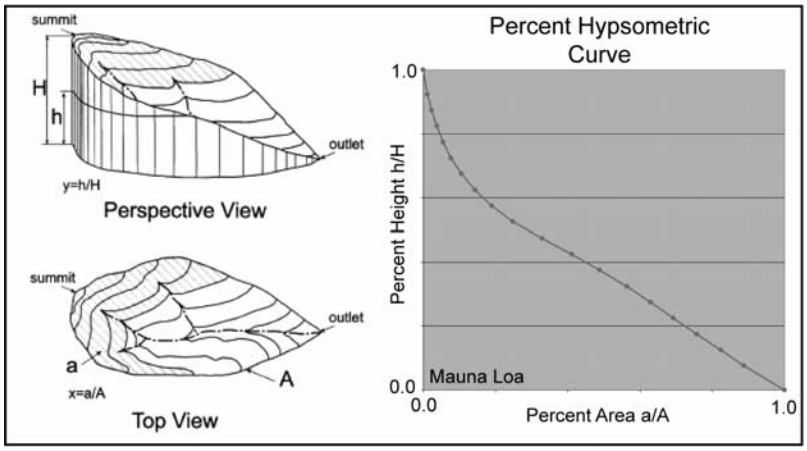

Figure 2. Schematic diagram showing the variables used to derive a hypsometric curve (modified from *Strahler* [1952] and *Luo* [1998]). Total relief (H) is determined by subtracting the lowest elevation of the landscape from the maximum elevation. A = total projected area of the landscape; a = area of landscape that is higher than h; H = total relief of the landscape; h = height above the lowest elevation. An example of the hypsometric curve for Mauna Loa as determined with SRTM-1 data is shown on the right.

was the most important SRTM limitation, but found that the absolute vertical accuracy presents few problems for regional morphometric studies of topography and slope. Despite higher errors in areas of high relief and/or vegetation cover, the SRTM data products provide the best available, nearly global, topographic data set of the Earth [*Sun et al.*, 2003].

3. Methodology

[10] As stated by *Moore and Mark* [1992], the shield volcanoes that make up the island of Hawaii are particularly suitable to terrain analysis because they are young, relatively simple volcanic environments displaying a limited range of rock types and associated modes of formation, as compared to other landscapes. The SRTM data provide the opportunity to test new terrain analysis techniques on the five Hawaiian volcanoes, while establishing a basis for the possibility of future analyses of other volcanoes using these data. We conducted our studies for each subaerial Hawaiian shield based on the mapped volcano boundaries of *Wolfe and Morris* [1996] (Figure 1).

[11] We determined average and median slope values using the version 2 (Finished data), 1 and 3 arc sec SRTM data (hereinafter referred to as SRTM-1 and SRTM-3, respectively) with spatial resolutions of 30 and 90 m (although *Guth* [2006] states that the SRTM-1 resolution might be closer to 2 arc sec (60 m) with regard to visual quality and terrain information). We derived a grid of slope values from both SRTM DEMs with the ArcGIS 9.2 (by ESRI) Spatial Analyst slope function (described by *Burrough and McDonell* [1998] and *Longley et al.* [2001]). We produced slope histograms from which we determined each shield's average and median slope value, as was done by *Moore and Mark* [1992] using previously available DEM data.

[12] The hypsometric curve of a landscape describes the area-altitude relation or the distribution of area versus relief [*Luo*, 2000]. *Strahler* [1952] introduced the relative hypsometric curve to relate the normalized cross-sectional area of a drainage basin to the relative height above a base level. The hypsometric curve is a plot of the height of each contour interval expressed as a proportion of the full height of the terrain (y axis) relative to its area as a proportion of the total area of the terrain (x axis) (Figure 2) [*Luo*, 1998]. The hypsometric integral (HI) is a measure of the distribution of landmass within the landscape [*Strahler*, 1952] and is determined as the ratio of area beneath the hypsometric curve. Changes in the shape of the curve, and the related integral, describe the relationship between constructive and destructive processes active on the surface [*Strahler*, 1958; *Weissel and Pratson*, 1994].

[13] We extracted the topography of each shield from the SRTM-1 DEM and calculated its area within 20 elevation bands each representing 5% of the total relief of the shield. We calculated the cumulative area per elevation band from the highest to the lowest elevation so that the area represented by the lowest band is equal to the total area of the shield. In this way, the cumulative area per band represents the area of that elevation and all of the topography above it. We normalized the cumulative area (a) to the total area of the shield (A) and plotted these data against the elevation value for each bin (h) normalized to the shield's total elevation (H). The result is the hypsometric curve showing normalized height (h/H) relative to normalized surface area (a/A). The HI is calculated from the hypsometric curve plot by determining the area beneath the curve and dividing it by the total area of the plot (Figure 2).

4. Results

[14] We calculated the average and median slope values for each volcano from the total number of slope measurements in the SRTM grids. Table 1 shows our results from SRTM-1 and SRTM-3 in comparison with the average slopes determined by *Moore and Mark* [1992]. SRTM derived average and median slopes increase with increased volcano age, matching well with the trend shown by the results from *Moore and Mark* [1992] (Figure 3). SRTM-3 slopes are consistently lower than their SRTM-1 equivalents by 0.4 to 0.7°.

Table 1. SRTM-Derived Median and Average Slope Values for the Subaerial Hawaiian Shield Volcanoes for Comparison With the Values Presented by *Moore and Mark* [1992]

Volcano	SRTM-1 Median Slope Value (deg)	SRTM-1 Average Slope Value (deg)	SRTM-3 Median Slope Value (deg)	SRTM-3 Average Slope Value (deg)	*Moore and Mark* [1992] Slope Value (deg)
Kilauea	2.9	3.8	2.3	3.2	3.3
Mauna Loa	5.2	5.8	4.8	5.3	5.4
Hualalai	5.8	6.8	5.4	6.2	6.6
Mauna Kea	6.4	7.4	5.7	6.7	7.0
Kohala	7.2	10.1	6.7	9.3	11.3

[15] The average slopes are ~1° higher than the median values except for Kohala, where the differences are 2.6° (SRTM-3) and 2.9° (SRTM-1). *Moore and Mark* [1992] and *Rowland and Garbeil* [2000] showed that higher than average slope values for Kohala and Kilauea are often associated with mass movements and fluvial erosion. Removal of the atypically high slopes from the Kohala and Kilauea slope grids in this study resulted in decreases in median slope for Kilauea by 0.1° in both data sets. The median slope for Kohala decreased by 0.4° while the average slope decreased by 2.5° (SRTM-1) and 2.4° (SRTM-3). The decrease in average slope results in differences of 0.8° (SRTM-1) and 0.6° (SRTM-3) with median slopes for Kohala, which are comparable to the difference between median and average slope for the other shield volcanoes.

[16] We conducted hypsometric analyses on the SRTM-1 data to derive the hypsometric curve and integral (HI) for each shield as a measurement of how each volcano's relief is distributed throughout its surface area. With the exception of Kilauea, the curves generally form an S-shaped pattern with a transition from concave to convex up from the left to right, as best exemplified by Mauna Loa (Figure 3). Kilauea maintains a slight concave pattern across the plot. There is no clear progression among the curves related to shield age. The HI values increase slightly among Kilauea, Mauna Loa, and Hualalai (Figure 4). Mauna Kea shows a break from this trend with a decrease compared to the other shields, while Kohala shows the largest HI value.

5. Discussion

5.1. Slopes

[17] A slope image derived from the SRTM-1 data for the island of Hawaii is shown in Figure 1. *Moore and Mark* [1992] and *Rowland and Garbeil* [2000] provide detailed descriptions of the relationship between slope and elevation for these volcanoes. Here we compare average and median slope values determined from SRTM data with the results of *Moore and Mark* [1992] to test the usability of SRTM data and to examine the role of data resolution.

[18] *Moore and Mark* [1992] showed an increase in average slope with volcano age. We plotted their values on Figure 3 for comparison with our SRTM-derived slope results. The slope plot shows a fairly simple progression from Kilauea to Kohala, associated with an increase in average and median slope, showing that younger shields are typified by lower slopes. The trend in average slopes from *Moore and Mark* [1992] matches well with the trend in average and median slopes that we derived from SRTM data

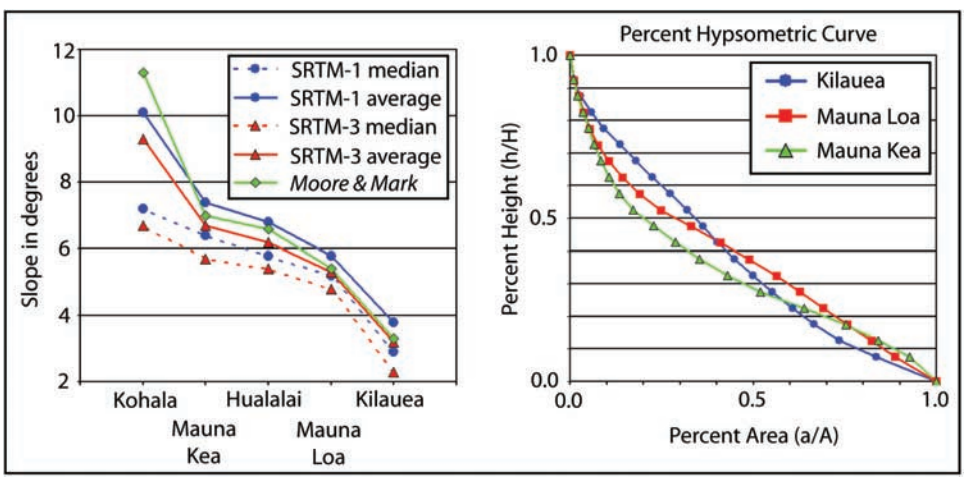

Figure 3. The plot on the left shows the average and median slope values for each Hawaiian volcano derived from SRTM data with respect to volcano age. For comparison, the green line shows the average slope data presented by *Moore and Mark* [1992]. The plot on the right shows the hypsometric curves for Kilauea, Mauna Loa, and Mauna Kea. Hualalai and Kohala are omitted for ease of visual comparison. However, their hypsometric integrals are presented in Figure 4, which is a quantitative representation of the hypsometric curve.

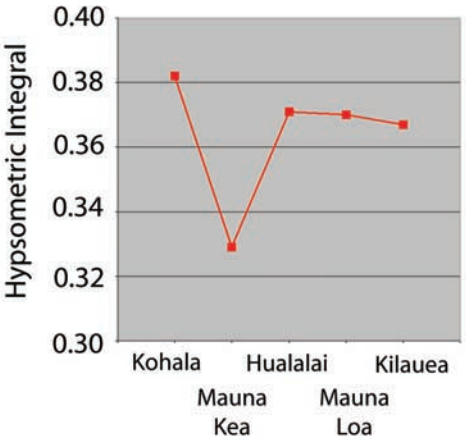

Figure 4. A plot showing the hypsometric integral for the Hawaiian shield volcanoes as derived from SRTM-1 data plotted against volcano age.

between Kilauea and Mauna Kea. The average slope presented by *Moore and Mark* [1992] shows a larger increase in slope between Kohala and Mauna Kea than do the average SRTM slopes. The difference results from the two unique types of data used for each study. SRTM data contain some voids over steep slopes due to radar shadowing and foreshortening [*Hall et al.*, 2005; *Crippen et al.*, 2007; *Luedeling et al.*, 2007; *Farr et al.*, 2007]. The steep, eroded slopes of Kohala did produce some SRTM data voids. The lack of these high slope values acts to decrease Kohala's slope values derived from SRTM data relative to the DEM data used by *Moore and Mark* [1992], which were derived from USGS 7.5-min quadrangles. This result suggests that SRTM data are less sensitive to changes in volcano shape that result from erosion after a volcano passes beyond the alkalic capping stage.

[19] The median slopes that we derived from SRTM data are consistently lower than the average slopes, and the medians do not display the same sharp slope increase from Mauna Kea to Kohala that is seen in the average slope values. *Kreslavsky and Head* [1999, 2000] suggest that average slope might not be the best measure of a surface because gridded topographic data typically have infrequent, anomalously high slope values within a given region. The median is less sensitive to these rare values than is the average. As a result, average slope values for the four youngest shields are $\sim 1°$ higher than the median slope values. Kohala is an exception with average slopes that are 2.6° to 2.9° higher than the median slopes. Kohala also displays the highest slopes on the island within its eroded valleys [*Moore and Mark*, 1992; *Rowland and Garbeil*, 2000], thereby creating a larger difference between its median and average, which is more sensitive to these relatively rare high slope areas.

[20] A comparison among the different data sets shows that slopes decrease with coarser DEM resolution. This is to be expected as a decrease in data resolution increases the baseline along which slope is calculated [*Hodgson*, 1995; *Kienzle*, 2004]. Although slope values derived from the coarser resolution SRTM-3 data are lower than those from the SRTM-1 data, the plots show the same trend related to shields at different stages of development. The consistency in trends between the data sets shows that both 1 and 3 arc sec data reveal the effects of surface forming processes at comparable scales. Therefore, similar studies can be conducted on other shield volcanoes outside the United States using the 3 arc sec SRTM data.

5.2. Hypsometry

[21] We conducted hypsometric analyses on the SRTM-1 DEM. In the case of a shield volcano, changing relief and surface area are dominantly controlled by volcanic construction, subsidence, and erosion. Because the relief-surface area ratio controls the shape of the hypsometric curve, hypsometry provides insight into each volcano's history of volcanic construction, subsidence, and erosion. Relative to the range of HI values calculated by *Strahler* [1952] to describe the development of drainage basins (>0.600 is considered to be in an inequilibrium stage and 0.400 to 0.600 is considered in an equilibrium stage), the Hawaiian shields display a much smaller range of 0.053 between 0.329 at Mauna Kea and 0.382 at Kohala (Figure 4).

[22] Similar HI values for younger Hawaiian volcanoes suggest that shield growth maintained a relatively constant ratio of relief to surface area through the early stages of alkalic capping (Hualalai). The ratio is different at Mauna Kea. As eruptions became more silica-rich, viscous, and gas-rich than during the younger tholeiitic stage [*Moore and Mark*, 1992; *Wolfe et al.*, 1997], flows tended to accumulate near the summit thereby increasing relief. As flow lengths shortened, presumably associated with a cessation of rift eruptions at Mauna Kea [*Wolfe et al.*, 1997], the surface area of the shield stopped increasing. The result was a change in the ratio of relief to surface area relative to the younger volcanoes, causing the measured HI value to decrease sharply. As subsidence and erosion became the dominant processes at Kohala, the low slope, lower flanks were submerged beneath the ocean. The reduction of total surface area occurred at a faster rate relative to the subsidence-driven reduction in relief, which increases the measured HI value relative to Mauna Kea. Similar to average and median slope trends [*Moore and Mark*, 1992], the most significant changes in hypsometry are related to the volcano (Mauna Kea) that is currently in the advanced stages of alkalic capping associated with more pronounced effects from subsidence and erosion relative to the younger volcanoes.

[23] The detailed shape of the hypsometric curve also supports inferences based on the HI and are most easily seen when comparing Kilauea, Mauna Loa, and Mauna Kea (Figure 3). Kilauea shows an even distribution of relief to surface area expressed as a slight concave up curve. Over the last 100 ka, eruption rates for Mauna Loa have steadily declined and eruption centers along the rift zones have migrated toward the summit [*Lipman*, 1995; *Lipman and Moore*, 1996]. Although the HI indicates that the relief per area for Mauna Loa is comparable to that of Kilauea, the gradual addition of relief in the upper elevations (higher slopes) causes the hypsometric curve to drop below that of Kilauea at high elevations (h/H) while rising above that for Kilauea at lower elevations (h/H). This trend continues into the alkalic capping phase producing a more pronounced S-shaped curve for Mauna Kea than for that of Mauna Loa.

[24] In summary, average and median slopes and hypsometric integrals calculated from SRTM data show that a suite of terrain analyses can be used to quantify a change in Hawaiian shield morphology related to changes in eruptive and erosive processes. Average and median slope values derived from SRTM data show a similar trend to that reported by *Moore and Mark* [1992], indicating that older shields are steeper. The same trends are seen in both the SRTM-1 and the nearly global SRTM-3 data, enabling comparison with other volcanoes outside the United States. Hypsometric analyses show that the subaerial Hawaiian shields maintain a consistent relationship between relief and surface area when compared to landscapes dominated by tectonic uplift and erosion. The most significant change in the hypsometric curve occurs once alkalic capping and subsidence alter the relationship between vertical and lateral growth of the shields.

5.3. Implications

[25] The terrain analyses presented here demonstrate an increase in subaerial slope, and the relief-surface area ratio, with increased age of the Hawaii shields. These results are consistent with other terrain analyses [*Mark and Moore*, 1987; *Moore and Mark*, 1992; *Rowland and Garbeil*, 2000], from which the change in morphology was quantified and attributed to the balance between the changing style of volcanic construction (e.g., eruptive style) and erosive destruction. However, using the evolution of the Hawaiian shields as a framework for interpreting other volcanic systems from remotely sensed data alone can also be linked with lava flow mapping and extended to provide additional insight into the internal dynamics of other volcanoes.

[26] Increased slope and relief-surface area ratios for the Hawaiian shields are associated with a change in lava flow structures. Mapping shows that ~58–67% of the surface of Kilauea was emplaced via tube-fed flows, compared to ~30% at Mauna Loa [*Greeley*, 1987; *Holcomb*, 1987; *Lockwood and Lipman*, 1987]. Some tubes appear to have developed on Hualalai [*Kauahikaua et al.*, 2002], but no total estimate of the current surface emplaced via tubes is published. Observations of active Hawaiian flows show that tubes tend to form during long-lived, stable eruptions at low to moderate effusion rates, whereas channels tend to develop during shorter-lived, unstable eruptions at moderate to high effusion rates [*Greeley*, 1987; *Holcomb*, 1987; *Rowland and Walker*, 1990; *Peterson et al.*, 1994; *Heliker et al.*, 1998; *Kauahikaua et al.*, 1998, 2003]. Lava tubes tend to produce longer flows than open channels in part because they thermally insulate the lava [*Swanson*, 1973; *Keszthelyi*, 1995; *Sakimoto and Zuber*, 1998, *Helz et al.*, 2003] and because they are the product of longer-lived, stable, low effusion rate eruptions relative to channel-forming events. Therefore, a higher abundance of tubes will typically produce less relief (lower slopes), while increasing surface area, than shorter channel-fed flows, some of which accumulate nearer to their vents than typically longer tube-fed flow fields. Mapping combined with terrain analyses of remotely sensed data can establish this relationship for comparison with terrain analyses.

[27] Magma production is in part a control on the style of a volcanic eruption. Average magma production rates of 0.1 km^3/a [*Dvorak and Dzurisin*, 1993] or higher (0.18 km^3/a [*Cayol et al.*, 2000]) are estimated for younger Hawaiian shield volcanoes, decreasing to as low as 0.0004 km^3/a as they progress into the alkalic capping stage [*Lipman*, 1995; *Wolfe et al.*, 1997]. The decline in magma production decreases the frequency of eruptions, as well as effusion rates and durations during those eruptions. Eruptions at high rates are typically short-lived as they rapidly remove volume from the magma chamber, reducing the driving pressure [*Decker*, 1987]. Low eruption rates typify long-lived eruptions, emplacing volumes of magma much greater than the presumed volume of the underlying chamber. Therefore, long-lived eruptions require a steady supply of magma from below the chamber or buffered eruption conditions [*Decker*, 1987; *Parfitt and Head*, 1993]. These long-lived, stable eruption conditions favor tube formation. Therefore, an increase in flank slope and relief-surface area ratio, and a change from tube- to channel-forming eruptions as determined from remote sensing data can be used to qualitatively suggest a decrease in magma production (Figure 5).

6. Conclusions

[28] The SRTM data enable the application of terrain analyses to the Hawaiian shield volcanoes. Previous terrain analyses applied to the Hawaiian volcanoes included determination of average slope values [*Moore and Mark*, 1992] and average slope-elevation studies [*Mark and Moore*, 1987; *Moore and Mark*, 1992; *Rowland and Garbeil*, 2000] based on multiple data sets as they became available. We compared the trend between average and median slope values for the subaerial Hawaiian shield volcanoes with past work [*Moore and Mark*, 1992] and conducted hypsometric analyses using the SRTM DEM data. Average and median slope values when plotted against volcano age match well with the data presented by *Moore and Mark* [1992], suggesting that SRTM data are suitable for conducting terrain analyses on the Hawaiian shield volcanoes. Differences between the trends in SRTM derived values and *Moore and Mark*'s [1992] results are attributed to radar shadows in steep regions within the SRTM data sets that are not present in the 7.5-min quadrangle data, thereby decreasing the slope values for Kohala when measured with SRTM. SRTM-3 data consistently produce lower slope values compared to the SRTM-1 data as is expected of coarser resolution data but produce the same trend as displayed by the higher resolution SRTM-1, suggesting that both data lead to comparable conclusions.

[29] Hypsometric analyses indicate that shield growth maintains a relatively constant relief-surface area ratio through the early stages of alkalic capping. During the alkalic capping phase a volcano's relief increases while its lateral growth ceases and begins to decrease as the volcano's low slope distal margins are slowly submerged. The result is a dramatic drop in the hypsometric integral. After alkalic capping ceases (e.g., Kohala) the volcano's upward growth stops as surface area continues to decrease. As a result, the ratio of surface area to relief returns to the same trend shown by younger volcanoes that are growing both vertically and laterally. Therefore, hypsometric studies of the Hawaiian shields are most sensitive to the transition from late alkalic capping to erosion when the relief-surface

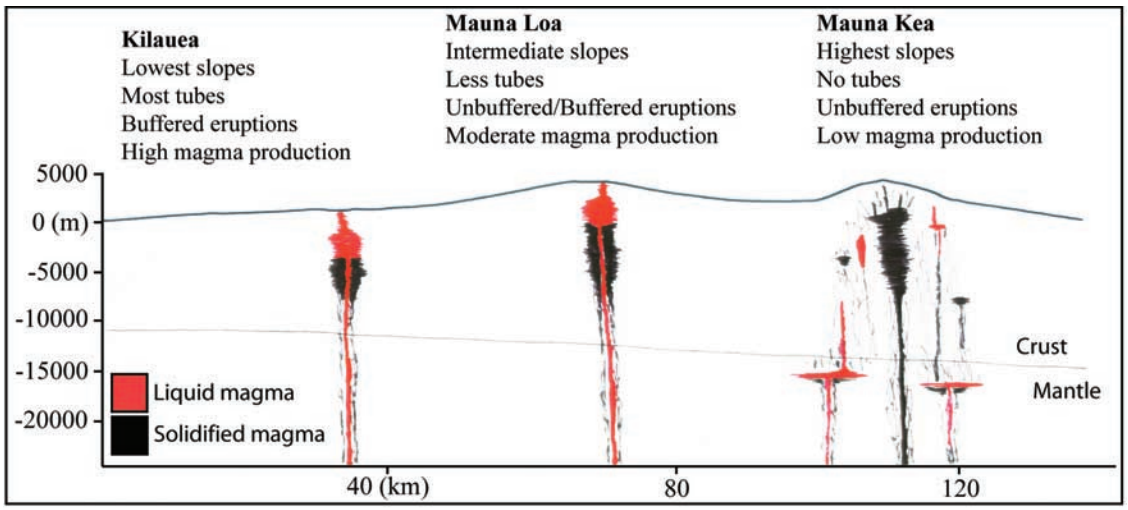

Figure 5. A stylized cross section based on the cross sections of *Wolfe et al.* [1997] and derived from SRTM-1 data showing Kilauea, Mauna Loa, and Mauna Kea. Average and median slope values and hypsometry analyses demonstrate quantitatively an increase in volcano slope associated with age. The abundance of lava tubes also decreases with shield age, which can be determined by mapping of remotely sensed data. These changes are in part controlled by changes in eruptive style [*Mark and Moore*, 1987; *Moore and Mark*, 1992; *Rowland and Garbeil*, 2000], which is related to the magma production rate for each volcano.

area ratio is most impacted by the interaction of volcanic and erosive processes.

[30] SRTM data produce comparable average and median slope results to those of *Moore and Mark* [1992], and SRTM-1 and SRTM-3 produce comparable results to one another. SRTM-3 data, which cover regions outside the United States, can be used to conduct similar terrain analyses on remote volcanoes for which field work might not be a possibility. Increases in flank slope and relief-surface area ratio, and a change from tube- to channel-forming eruptions as determined from terrain analyses and mapping of remote sensing data, can be thought of as indicators of a decrease in magma production. Therefore, the combination of average and median slope, average slope-elevation [*Mark and Moore*, 1987; *Moore and Mark*, 1992; *Rowland and Garbeil*, 2000], and hypsometric analyses can be used together with lava flow mapping to provide insight into a volcano's eruption and magma production history for remote terrestrial volcanoes or volcanoes on other planets.

[31] **Acknowledgments.** The authors would like to thank D. A. Williams and W. B. Garry for providing useful reviews of the manuscript and R. Arrowsmith for providing insight into this study. We also thank L. Keszthelyi, S. Fagents, and an anonymous reviewer for comments that improved this paper. This research was supported by NASA Planetary Geology and Geophysics (PG&G) grant NAG5-13153, NASA Graduate Student Research Program (GSRP) grant NGT5-145, and a NASA Postdoctoral Program (NPP) fellowship administered through Oak Ridge Associated Universities at Goddard Space Flight Center.

References

Burrough, P. A., and R. A. McDonell (1998), *Principles of Geographical Information Systems*, 2nd ed., 356 pp., Oxford Univ. Press, New York.

Carabajal, C. C., and D. J. Harding (2005), ICESat validation of SRTM C-band digital elevation models, *Geophys. Res. Lett.*, *32*, L22S01, doi:10.1029/2005GL023957.

Cayol, V., J. H. Dieterich, A. T. Okamura, and A. Miklius (2000), High magma storage rates before the 1983 eruption of Kilauea, Hawaii, *Science*, *288*, 2343–2346, doi:10.1126/science.288.5475.2343.

Clague, D. A., and G. B. Dalrymple (1987), The Hawaiian-Emperor volcanic chain; Part I, Geologic evolution, in *Volcanism in Hawaii*, edited by R. W. Decker et al., *U.S. Geol. Surv. Prof. Pap.*, *1350*, 5–54.

Crippen, R. E., S. J. Hook, and E. J. Fielding (2007), Nighttime ASTER thermal imagery as an elevation surrogate for filling SRTM DEM voids, *Geophys. Res. Lett.*, *34*, L01302, doi:10.1029/2006GL028496.

Decker, R. W., (1987), Dynamics of Hawaiian volcanoes: An overview, in *Volcanism in Hawaii*, edited by R. W. Decker et al., *U.S. Geol. Surv. Prof. Pap.*, *1350*, 997–1018.

Dvorak, J. J., and D. Dzurisin (1993), Variations in magma supply rate at Kilauea Volcano, Hawaii, *J. Geophys. Res.*, *98*(B12), 22,255–22,268, doi:10.1029/93JB02765.

Falorni, G., V. Teles, E. R. Vivoni, R. L. Bras, and K. S. Amaratunga (2005), Analysis and characterization of the vertical accuracy of digital elevation models from the Shuttle Radar Topography Mission, *J. Geophys. Res.*, *110*, F02005, doi:10.1029/2003JF000113.

Farr, T. G., et al. (2007), The Shuttle Radar Topography Mission, *Rev. Geophys.*, *45*, RG2004, doi:10.1029/2005RG000183.

Greeley, R., (1987), The role of lava tubes in Hawaiian volcanoes, in *Volcanism in Hawaii*, edited by R. W. Decker et al., *U.S. Geol. Surv. Prof. Pap.*, *1350*, 1589–1605.

Guth, P. L. (2006), Geomorphometry from SRTM: Comparison to NED, *Photogramm. Eng. Remote Sens.*, *72*, 269–277.

Hall, O., G. Falconi, and R. L. Bras (2005), Characterization and quantification of data voids in the Shuttle Radar Topography Mission data, *IEEE Geosci. Remote Sens. Lett.*, *2*, 177–181, doi:10.1109/LGRS.2004.842447.

Heliker, C. C., M. T. Mangan, T. N. Mattox, J. P. Kauahikaua, and R. T. Helz (1998), The character of long-term eruptions: Inferences from episodes 50–53 of the Puu Oo-Kupaianaha eruption of Kilauea Volcano, *Bull. Volcanol.*, *59*, 381–393, doi:10.1007/s004450050198.

Helz, R. T., C. Heliker, K. Hon, and M. Mangan (2003), Thermal efficiency of lava tubes in the Puu Oo-Kupaianaha eruption, in *The Puu Oo-Kupaianaha Eruption of Kilauea Volcano, Hawaii, the First 20 Years*, edited by C. Heliker et al., *U.S. Geol. Surv. Prof. Pap.*, *1676*, 63–87.

Hodgson, M. E. (1995), What cell size does the computed slope/aspect angle represent?, *Photogramm. Eng. Remote Sens.*, *61*(5), 513–517.

Holcomb, R. T. (1987), Eruptive history and long-term behavior of Kilauea Volcano, in *Volcanism in Hawaii*, edited by R. W. Decker et al., *U.S. Geol. Surv. Prof. Pap.*, *1350*, 261–350.

Kauahikaua, J., K. V. Cashman, T. N. Mattox, C. C. Heliker, K. A. Hon, M. T. Mangan, and C. R. Thornber (1998), Observations on basaltic lava streams in tubes from Kilauea volcano, Island of Hawaii, *J. Geophys. Res.*, *103*(B11), 27,303–27,323, doi:10.1029/97JB03576.

Kauahikaua, J., K. V. Cashman, D. A. Clague, D. Champion, and J. T. Hagstrum (2002), Emplacement of the most recent lava flows on Hualalai

Volcano, Hawaii, *Bull. Volcanol.*, *64*, 229–253, doi:10.1007/s00445-001-0196-8.

Kauahikaua, J., D. R. Sherrod, K. V. Cashman, C. Heliker, K. Hon, T. N. Mattox, and J. A. Johnson (2003), Hawaiian lava-flow dynamics during the Puu Oo-Kupaianaha eruption: A tale of two decades, in *The Puu Oo-Kupaianaha Eruption of Kilauea Volcano, Hawaii, the First 20 Years*, edited by C. Heliker et al., *U.S. Geol. Surv. Prof. Pap.*, *1676*, 63–87.

Keszthelyi, L. (1995), A preliminary thermal budget for lava tubes on the Earth and planets, *J. Geophys. Res.*, *100*(B10), 20,411–20,420, doi:10.1029/95JB01965.

Kienzle, S. (2004), The effect of DEM raster resolution on first order, second order and compound terrain derivatives, *Trans. GIS*, *8*(1), 83–111, doi:10.1111/j.1467-9671.2004.00169.x.

Kreslavsky, M. A., and J. W. Head III (1999), Kilometer-scale slopes on Mars and their correlation with geologic units: Initial results from Mars Orbiter Laser Altimeter (MOLA) data, *J. Geophys. Res.*, *104*(E9), 21,911–21,924, doi:10.1029/1999JE001051.

Kreslavsky, M. A., and J. W. Head III (2000), Kilometer-scale roughness of Mars: Results from MOLA data analysis, *J. Geophys. Res.*, *105*(E11), 26,695–26,711, doi:10.1029/2000JE001259.

Lipman, P. W. (1995), Declining growth of Mauna Loa during the last 100000 years: Rates of lava accumulation vs. gravitational subsidence, in *Mauna Loa Revealed; Structure, Composition, History, and Hazards*, *Geophys. Monogr. Ser*, vol. 92, edited by J. M. Rhodes and J. P. Lockwood, pp. 45–80, AGU, Washington, D. C.

Lipman, P. W., and J. G. Moore (1996), Mauna Loa lava accumulation rates at the Hilo drill site: Formation of lava deltas during a period of declining overall volcanic growth, *J. Geophys. Res.*, *101*(B5), 11,631–11,641, doi:10.1029/95JB03214.

Lockwood, J. P., and P. W. Lipman (1987) Holocene eruptive history of Mauna Loa Volcano, in *Volcanism in Hawaii*, edited by R. W. Decker et al., *U.S. Geol. Surv. Prof. Pap.*, *1350*, 509–536.

Longley, P. A., M. F. Goodchild, D. J. Maguire, and D. W. Rhind (2001), *Geographic Information Systems and Science*, 454 pp., John Wiley, New York.

Luedeling, E., S. Siebert, and A. Buerkert (2007), Filling the voids in the SRTM elevation model–A TIN-based delta surface approach, *J. Photogramm. Remote Sens.*, *62*, 283–294, doi:10.1016/j.isprsjprs.2007.05.004.

Luo, W. (1998), Hypsometric analysis with a geographic information system, *Comput. Geosci.*, *24*(8), 815–821, doi:10.1016/S0098-3004(98)00076-4.

Luo, W. (2000), Quantifying groundwater-sapping landforms with a hypsometric technique, *J. Geophys. Res.*, *105*(E1), 1685–1694, doi:10.1029/1999JE001096.

Mark, R. K., and J. G. Moore (1987), Slopes of the Hawaiian Ridge, in *Volcanism in Hawaii*, edited by R. W. Decker et al., *U.S. Geol. Surv. Prof. Pap.*, *1350*, 101–108.

Moore, J. G., and R. K. Mark (1992), Morphology of the Island of Hawaii, *GSA Today*, *2*(11), 257–262.

Parfitt, E. A., and J. W. Head III (1993), Buffered and unbuffered dike emplacement on Earth and Venus: Implications for magma reservoir size, depth, and rate of magma replenishment, *Earth Moon Planets*, *61*(3), 249–281, doi:10.1007/BF00572247.

Peterson, D. W., and R. B. Moore (1987), Geologic history and evolution of geologic concepts, Island of Hawaii, in *Volcanism in Hawaii*, edited by R. W. Decker et al., *U.S. Geol. Surv. Prof. Pap.*, *1350*, 149–190.

Peterson, D. W., R. T. Holcomb, R. I. Tilling, and R. L. Christiansen (1994), Development of lava tubes in the light of observations at Mauna Ulu, Kilauea Volcano, Hawaii, *Bull. Volcanol.*, *56*, 343–360.

Pike, R. J. (2000), Geomorphometry–diversity in quantitative surface analysis, *Prog. Phys. Geogr.*, *24*, 1–20.

Rabus, B., M. Eineder, A. Roth, and R. Barnler (2003), The Shuttle Radar Topography Mission–A new class of digital elevation models acquired by spaceborne radar, *J. Photogramm. Remote. Sens.*, *57*, 241–262, doi:10.1016/S0924-2716(02)00124-7.

Rodriguez, E., C. S. Morris, J. E. Belz, E. C. Chapin, J. M. Martin, W. Daffer, and S. Hensley (2005), An assessment of the SRTM topographic products, *Tech. Rep. JPL D-31639*, 143 pp., Jet Propulsion Lab, Pasadena, Calif.

Rodriguez, E., C. S. Morris, and J. E. Belz (2006), A global assessment of the SRTM performance, *J. Photogramm. Remote Sens.*, *72*(3), 249–260.

Rowland, S. K., and H. Garbeil (2000), Slopes of oceanic basalt volcanoes, in *Remote Sensing of Active Volcanism*, *Geophys. Monogr. Ser*, vol. *116*, edited by P. J. Mouginis-Mark et al., AGU, Washington, D. C.

Rowland, S. K., and G. P. L. Walker (1990), Pahoehoe and aa in Hawaii: Volumetric flow rate controls the lava structure, *Bull. Volcanol.*, *52*, 615–628, doi:10.1007/BF00301212.

Sakimoto, S. E. H., and M. T. Zuber (1998), Flow and convection cooling in lava tubes, *J. Geophys. Res.*, *103*(B11), 27,465–27,487, doi:10.1029/97JB03108.

Strahler, A. N. (1952), Hypsometric (area-altitude) analysis of erosional topography, *Geol. Soc. Am. Bull.*, *63*, 1117–1142, doi:10.1130/0016-7606(1952)63[1117:HAAOET]2.0.CO;2.

Strahler, A. N. (1958), Dimensional analysis applied to fluvial eroded landforms, *Geol. Soc. Am. Bull.*, *69*, 279–299, doi:10.1130/0016-7606(1958)69[279:DAATFE]2.0.CO;2.

Sun, G., K. J. Ranson, V. I. Kharuk, and K. Kovacs (2003), Validation of surface height from shuttle radar topography mission using shuttle laser altimeter, *Remote Sens. Environ.*, *88*, 401–411, doi:10.1016/j.rse.2003.09.001.

Swanson, D. A. (1973), Pahoehoe flows from the 1969–1971 Mauna Ulu eruption, Kilauea Volcano, Hawaii, *Geol. Soc. Am. Bull.*, *84*, 615–626, doi:10.1130/0016-7606(1973)84<615:PFFTMU>2.0.CO;2.

Tilling, R. I., and J. J. Dvorak (1993), Anatomy of a basaltic volcano, *Nature*, *363*, 125–133, doi:10.1038/363125a0.

Weissel, J. K., and L. F. Pratson (1994), The length-scaling properties of topography, *J. Geophys. Res.*, *99*(B7), 13,997–14,012, doi:10.1029/94JB00130.

Wilson, J. P., and J. C. Gallant (2000), Digital terrain analysis, in *Terrain Analysis*, edited by J. P. Wilson and J. C. Gallant, pp. 1–19, John Wiley, New York.

Wolfe, E. W., and J. Morris (1996), Geologic map of the Island of Hawaii, scale 1:100,000, *U. S. Geol. Surv. Misc. Invest. Map, I-2524-A*.

Wolfe, E. W., W. S. Wise, and G. B. Dalrymple (1997), The geology and petrology of Mauna Kea Volcano, Hawaii–A study of postshield volcanism, *U. S. Geol. Surv. Prof. Pap.*, *1557*, 129 pp.

J. E. Bleacher, Planetary and Geodynamics Laboratory, NASA Goddard Space Flight Center, Greenbelt, MD 20771, USA. (jacob.e.bleacher@nasa.gov)

R. Greeley, School of Earth and Space Exploration, Arizona State University, Tempe, AZ 85287-1404, USA.